

## THICKNESS AND ANNEALING EFFECTS ON THE STRUCTURAL AND OPTICAL CONDUCTIVITY PARAMETERS OF ZINC PHTHALOCYANINE THIN FILMS

S. R. ALHARBI<sup>a</sup>, A. F. QASRAWI<sup>b,c,\*</sup>, N. M. KHUSAYFAN<sup>a</sup>

<sup>a</sup>*Department of Physics, Faculty of Science, University of Jeddah, Jeddah, Saudi Arabia*

<sup>b</sup>*Department of Physics, Arab American University, Jenin, Palestine*

<sup>c</sup>*Group of physics, Faculty of Engineering, Atilim University, 06836 Ankara, Turkey*

In this work, the effects of the thin film thicknesses on the structural, optical absorption, energy band gap, dielectric spectra and optical conductivity parameters of the Zinc phthalocyanine thin films are considered. Thin films of ZnPc of thicknesses of 50–600 nm which are coated onto glass substrates are observed to exhibit amorphous nature of growth. The polycrystalline monoclinic ZnPc phase of the films is obtained via annealing the films at 200 °C in a vacuum atmosphere. Increasing the ZnPc films thickness shrunk the energy band gap in the B- and Q- bands and decreased both of the optical conductivities and free holes density in the Q-band. The increase in the film thickness is also observed to decrease the plasmon frequency and the drift mobility of holes in the films. The highest dielectric constant is obtained for films of thicknesses of 100 nm. The annealing process enhanced the optical absorption, redshifts the energy band gap value and the critical energy of the absolute maxima of dielectric constant. In addition, while the heat treatment enhanced both of the scattering times at femtosecond level and the drift mobility, it reduced the free holes density, and the plasmon frequency.

(Received February 15, 2020; Accepted May 18, 2020)

*Keywords:* ZnPC, X-ray diffraction, Plasmon, Drift mobility, Optical conductivity

### 1. Introduction

Phthalocyanine (ZnPc) is one of the promising organic materials that find its location in organic thin film transistors (TFT) technology. Recent reports indicated that these materials which can be grown onto flexible substrates are regarded as of low cost and of large area which make it attractive for optoelectronic designs including liquid crystal displays and organic light emitting diodes [1]. ZnPc TFT devices are known for their high stability and highly efficient luminance material. Such type of organic thin film transistors is observed to exhibit a photoresponsivity of 11.3 A/W when irradiated with light of intensity of 5  $\mu\text{W}/\text{cm}^2$  at 540 nm [2]. One novel property of these types of organic polymers is their ability to exhibit self-encapsulation to reveal ultracompact TFT with low biasing voltage [3]. It is also mentioned that, when excited with light of wavelengths of 351 nm, the ITO/ZnPc/Al/ZnPc/Cu TFT structure can exhibit an abrupt increase in the current values. For this transistor, the photoresponsivity reached 5.3 A/W [4]. In addition, ZnPc transistors which are prepared onto a dielectric configuration composed of Al<sub>2</sub>O<sub>3</sub>/poly(vinyl alcohol PVA)/poly(methyl) methacrylate (PMM) displayed high responsivity values up to  $9.7 \times 10^4$  A/W [5].

In spite of its ultrahigh responsivity compared to inorganic thin film transistors, ZnPc based devices suffers from the low mobility of charge carriers. The charge carrier mobility of the Al<sub>2</sub>O<sub>3</sub>/PVA/(PMM)/ZnPc is in the range of  $10^{-2}$ - $10^{-3}$  cm<sup>2</sup>/Vs [5]. Those of organic PQT-12 (poly(3, 3''- dialkylquaterthiophene) (PQT-12) polymer) based TFTs exhibit mobility values  $7.8 \times 10^{-2}$  cm<sup>2</sup>/Vs [2]. Even though these values are high compared to other organic thin film transistors,

---

\* Corresponding author: atef.qasrawi@aaup.edu

they are regarded as low in the world of TFT technology [6]. For this reason, here in this work, we will carry a complete analysis that gets use from the variation of the ZnPc layers thickness to reveal the best conditions for optical conduction. Particularly, thin layers of ZnPc thin films in the thickness range of 50-600 nm will be structurally and optically investigated to determine the relation between the structure and thickness of the films and between the thickness and optical conductivity parameters. The parameters which are presented by the drift mobility, the scattering time at femtosecond level, the free charge carrier density and the plasmon frequency will be determined from the dielectric spectral analysis in the visible region of light to determine the thickness which reveals the highest drift mobility value. The work will also consider the possible relation between the other optical and structural parameters and films thickness. Some of the samples will be subjected to an annealing process to attempt to enhance the structure and optimize better drift mobility values for ZnPc films.

## 2. Experimental details

Zinc phthalocyanine thin films of thicknesses of 50-600 nm are coated onto glass substrates using VCM-600 thermal evaporator under vacuum pressure of  $\sim 10^{-5}$  mbar. The source material was ZnPc (Alfa Aesar 99.9%) nano-powders. The powders are located in a boat like tungsten heater 10 cm below the substrate holder. The thickness of the films was measured with Inficon STM-2 thickness monitor which have resolution of 0.03 Å. The annealing of the 600 nm thick films were carried out in a vacuum media ( $10^{-4}$  mbar) at temperature of 200 °C for one hour. All the studied films were tested by the hot probe technique and were found to exhibit *p*-type conduction. The produced films are structurally characterized by MiniFlex-600 X-ray diffraction unit with scanning speed of 0.5°/min. The morphology of the films was tested by COXEM-200 scanning electron microscopes. The optical transmittance and reflectance spectra were measured with the help of thermoscientific Evolution 300 ultraviolet-visible light spectrophotometer in the spectral range of 300-1100 nm.

## 3. Results and discussion

In order to investigate the effect of the film thickness on the optical conductivity parameters of zinc phthalocyanine (ZnPc) thin films, we first attempt to explore the crystalline nature and morphology of the films. Fig. 1 illustrates the X-ray diffraction patterns for ZnPc thin films of thicknesses (*d*) of 50-600 nm. No intensive peaks are detected in the patterns of the as grown thin films in the studied thickness range. Such observation indicates the amorphous nature of the films. Earlier studies which take into account the thickness effect on the crystalline nature of the ZnPc thin films have shown that while thin films of thicknesses in the range of 100-250 nm exhibit amorphous nature, thicker films in the range of 300-1000 nm are of polycrystalline nature [7]. The obtained thin films were reported to be of monoclinic structure. The amorphous nature of the films and its crystallographic transitions are assigned to the elastic strain at the glass/film interfaces [7]. It is mentioned that for lower thicknesses ( $d < 250$  nm), the ZnPc films are elastically strained at the interface of the lattice of the film and the substrate. Increasing the thickness above 250 nm allowed the formation of misfit dislocations. These dislocations partially relaxes the film and allow the equilibrium free lattice parameters to be attained. This indication was supported by monitoring the intensity of the predominant peak ( $2\theta = 7.34^\circ$ ) which increased with increasing film thickness. In another work, ZnPc thin films of thicknesses of 750 nm are mentioned being of amorphous nature when grown at substrate temperature of 30° C. The crystalline phase at this thickness was achieved at substrate temperatures in the range of 50 °C-200 °C [8]. Ultrathin films of ZnPc whose thicknesses are in the range of 5-50 nm which are grown at substrate temperatures in the range of 30-90 °C are all observed to exhibit polycrystalline nature. For these films a triclinic ( $\alpha$ -ZnPc) or monoclinic ( $\gamma$ -ZnPc) phases are formed. The formation of the crystalline phase is reported to be independent from the kind of substrate, layer thickness, or substrate temperature [9]. From our observation and the reported literature data, it seems that identifying a

standard for the crystalline phase of ZnPc is not that easy. The crystallographic phase of ZnPc is randomly influenced by the thickness, substrate temperature and kind of substrate.

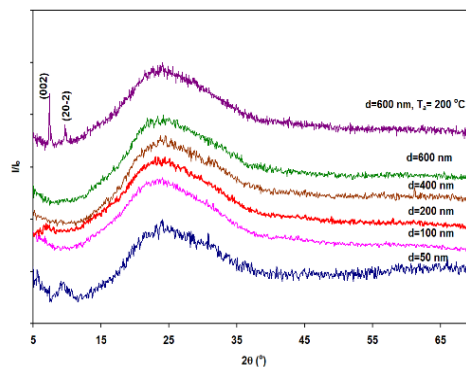


Fig. 1 The X-ray diffraction patterns for the ZnPc thin films at various thicknesses ( $d$ ) the indexed patterns are obtained after annealing of the ZnPc (600 nm) films at 200 °C for one hour in a vacuum.

In order to achieve polycrystalline phases of ZnPc thin films under study, the samples whose thicknesses are 600 nm were heat treated at ( $T_a$ ) 200 °C for one hour. The resulting XRD patterns are shown in Fig. 1. Two peaks centered at  $2\theta = 7.40^\circ$  and  $9.75^\circ$  were detected in the XRD patterns. To identify the crystalline phase of the annealed films “Crystdiff” software packages were employed to reproduce the experimental data. The simulator was tested for  $\alpha$  and  $\beta$ -phases of ZnPc assuming a respective lattice parameters of  $a = 25.9$ ,  $b = 3.8$ ,  $c = 23.9$  Å,  $\beta = 90.5^\circ$  and space group  $C_{2/c}$  and  $a = 19.274$ ,  $b = 4.8538$ ,  $c = 14.553$  Å,  $\beta = 120.48^\circ$  and space group  $P2_1a$  [10]. In accordance with the simulator, the strongest reflection of the monoclinic  $\beta$ -phase appears at  $2\theta = 5.32^\circ$  (100%) followed by  $2\theta = 6.31^\circ$  (69.9%),  $2\theta = 7.04^\circ$  (55.6%) and  $2\theta = 9.31^\circ$  (30.4%) along (100),  $(10\bar{1})$ , (001) and  $(20\bar{1})$  orientation directions, respectively. On the other hand, In the simulator,  $\alpha$ -phase displayed diffraction angles of  $2\theta = 6.82$ ,  $7.39$ ,  $10.02^\circ$  with relative intensity values percentages of 100%, 84.3% and 64.82%, respectively. While the first peak of the experimental data is closer to the theoretically estimated  $\alpha$ -phase, the second observed peak at  $2\theta = 9.75^\circ$  could be assigned to either  $\alpha$  or  $\beta$ -phase.

The calculated crystallite size ( $D$ ) from the maximum peak broadening ( $\bar{\beta}$ ) in accordance with Scherrer equation ( $D = 0.94\lambda/(\bar{\beta} \cos(\theta))$  [11]) reveals a crystallite size of value of 55 nm, microstrain ( $\epsilon = \bar{\beta}/(4\tan(\theta))$  [11]) value of  $1.01 \times 10^{-2}$  and defect density ( $\delta = \frac{15\epsilon}{bD}$  [11]), along the principle axis of the monoclinic phase  $b$ -axis, of  $7.11 \times 10^{11}$  lines/cm<sup>2</sup>. The structural parameters which are achieved via annealing process are somehow different from those reported in literature data assuring the variability in the structural formation process. A crystallite size, microstrain and defect density of values of 98.6 nm,  $3.68 \times 10^{-4}$  and  $1.03 \times 10^{11}$  lines/cm<sup>2</sup> were reported for ZnPc thin films of thicknesses of 750 nm [7]. On the other hand, trails to explore information about the thickness effect on the surface morphology of the ZnPc thin films failed owing to the amorphous nature of the films. The only obtainable scanning electron microscopy (SEM) images were for the thermally annealed films. The SEM image which was recorded from the surface of the annealed films is displayed in Fig. 2 (a). In accordance with the figure which represents an enlargement of 20000 times, the surface comprises randomly distributed grains of irregular shapes and average grain size of ~200 nm. The grain comprises at least four crystallites (assuming validity of X-ray diffraction calculations for crystallite size). Some grains exceed 350 nm in size. The larger the grain size, the higher the effective dielectric constant [12], the better the mobility [13], the better the thin film transistor characteristics [13]. Larger grain sizes are also important for optimizing higher photo-cell efficiencies [14].

The ZnPc thin films thickness on the optical transmittance ( $T$ ) is illustrated in Fig. 2 (b). It is clear from the transmittance spectra that there exist two high transmittance regions. For examples, for the films whose thicknesses are 50 nm,  $T$  values increases with increasing incident light wavelength ( $\lambda$ ) reaching a maxima of 84% at 440 nm. It then tends to remain constant in the wavelength range of 440-536 nm. In the  $\lambda$  domain of 536-692 nm,  $T$  values decreases with increasing  $\lambda$ . It then re-increase reaching a value of 84% at 800 nm, where it remains constant in the  $\lambda$  domain of 800-1100 nm. A significant effect of the samples thicknesses in the maximum transmittance regions (440-536 nm, 800-1100 nm) is observed. ZnPc is known to exhibit two transmittance edges in the B and Q band. While the B band is defined near 330 nm, the Q-band dominates near  $\lambda = 700$  nm [15]. It is clear from Fig. 2 (b), that the thicker the film, the more distinguishable the two bands. The thicker the film, the more redshift in the transmittance spectra. On the other hand, the reflectance spectra ( $R$ ) which is illustrated in Fig. 2 (c), did not show any systematic behavior as a response to the increased films thickness. In general the reflectance values are low and never exceed 20%. The local and absolute maximum reflectivity appears in the B and Q-bands, respectively. It is readable from Fig. 2 (b) and (c) that the highest reflectance value appears near 700 nm where the transmittance spectra show minima.

The measured transmittance and reflectance spectra are employed to determine the absorption coefficient ( $\alpha$ ) spectra through the relation ( $\alpha = 2.303(1 - T - R)/d$  [16]). This rule is used as the transmittance and reflectance arising from the glass substrates is removed through storing them in the system reference compartment and the multilayer effect are absent. The absorption coefficient spectra are shown in Fig. 2 (d).  $\alpha$  -spectra exhibit two strong absorption regions one in the B- band and the other is in the Q-band. It is clear from the figure that  $\alpha$  values decrease with increasing thickness and the absorption saturation region becomes wider as the thickness increases. As for examples, in the B-band region, while the  $\alpha$  -spectra exhibit no absorption saturation for the films of thickness of 50 nm and an absorption saturation region of 4.30-4.1 for the 100 nm thick sample, the absorption saturation appears in the range of 4.30-3.0 for the 400 and 600 nm thick samples. On the other hand, in the Q- band, the thinner the film, the sharper the absorption peak, the higher the absorption coefficient value. The decrease in the absorption coefficient values with increasing film thickness may be assigned to the involvement of the indirect photon transitions upon increased thickness [17]. It can also be assigned to the increased surface roughness with increasing film thickness [9, 17]. The rough the film surface, the larger the scattering, the less the ability of light absorption.

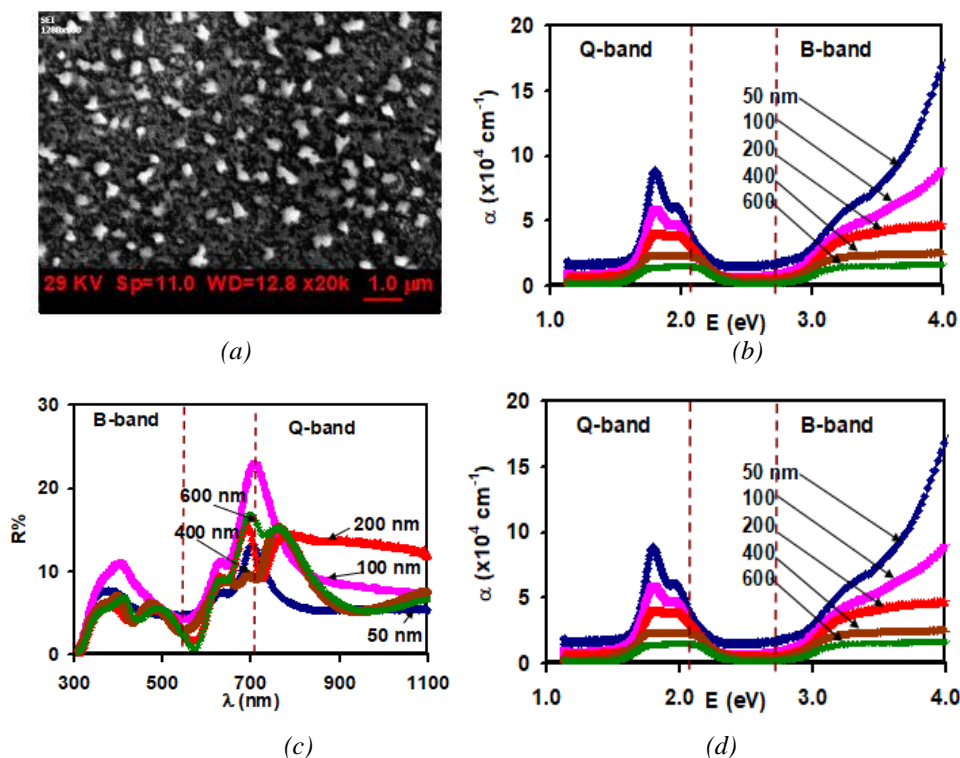


Fig. 2 (a) The scanning electron microscopy results, (b) the optical transmittance, (c) the optical reflectance and (d) the optical absorption coefficient for ZnPc thin films at various thicknesses.

Fig. 3 (a) illustrates a representative fitting of Tauc's equation  $((\alpha E)^2 \propto (E - E_g))$ [16] for direct allowed transitions. The  $E$ -axis crossings of the straight lines which appear in the figure lead to the determination of the thickness dependent energy band gaps ( $E_g$ ) which are shown in Fig. 3 (b) and (c) for the ZnPc films in the Q and B-bands, respectively. A significant decrease in the values of the energy band gap with increasing thickness can be observed from Fig. 3 (b) for the optical transitions in the Q-band. The slope of  $E_g - d$  variations reveals a negative rate of change ( $\delta E_g / \delta d$ ) of the band gap with thickness.  $\delta E_g / \delta d$  exhibits value of  $-1.72 \times 10^{-4} \text{ eV/nm}$ . The decrease in the values of the energy band gap with increasing film thickness was previously observed for the same films and was ascribed to the presence of internal electric fields associated with the defects present in the films [7, 15]. In contrast to the systematic behavior of  $E_g - d$  variations in the Q-band,  $E_g$  values initially decreased as  $d$  is increased to 400 nm and then slightly increased as  $d$  is increased further. In truth, the change in the values of the energy band gap is less pronounced compared to those observed in the Q-band. The highest  $E_g = 2.970 \text{ eV}$  value in B-band corresponds to  $d=50 \text{ nm}$ . The lowest value of  $E_g$  being  $2.895 \text{ eV}$  relates to  $d = 400 \text{ nm}$ .

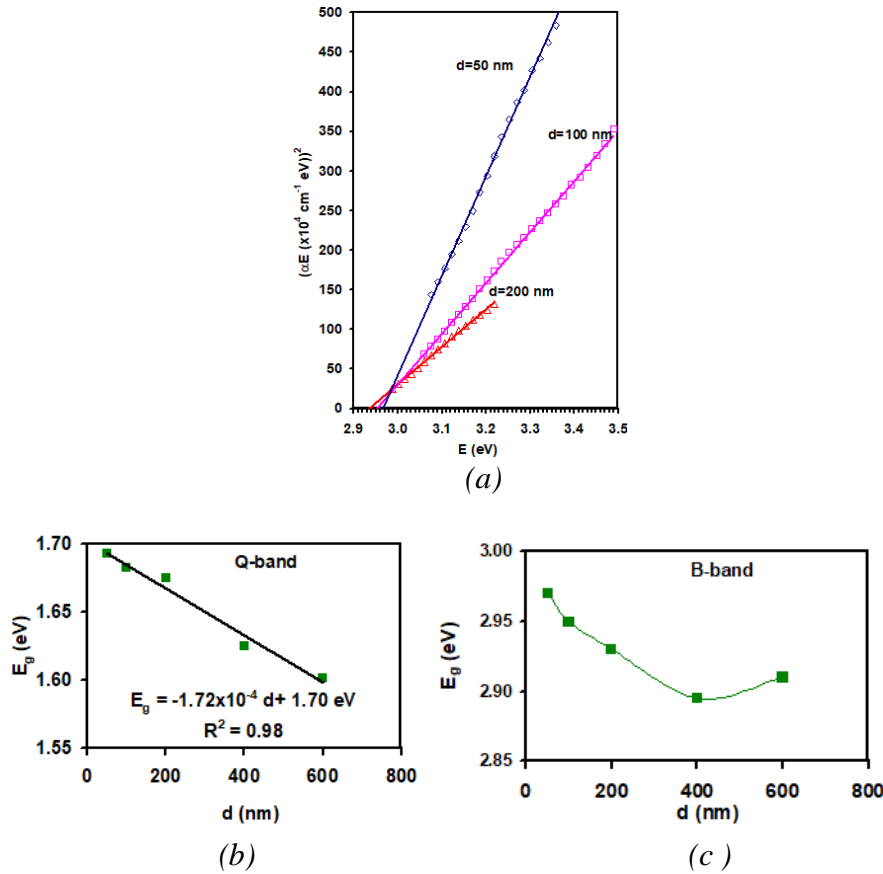


Fig. 3. (a) The Tauc's equation representative fittings, and the thickness dependent energy band gaps in the (b) B-band and (c) Q-band for ZnPc thin films.

As a main target of this work, we now attract the attention for the dielectric properties of the ZnPc thin films. The effective dielectric constant ( $\epsilon_{eff} = \epsilon_r + i\epsilon_{im}$ ) which allow finding to the real ( $\epsilon_r$ ) and imaginary ( $\epsilon_{im}$ ) parts of the dielectric constant are calculated from the refractive index ( $n$ ) and absorption coefficient spectra using the relations,  $\epsilon_{eff} = n^2$ ,  $\epsilon_r = n^2 - (\alpha\lambda/(4\pi))^2$  and  $\epsilon_{im} = 2n(\alpha\lambda/(4\pi))$  [16, 19]. The refractive index is determined from the measured transmittance, reflectance and absorption coefficient spectra at normal incidence using the relation,  $R = [(n-1)^2 + (\alpha\lambda/(4\pi))^2] / [(n+1)^2 + (\alpha\lambda/(4\pi))^2]$  [20, 21]. The imaginary part of the dielectric constant is used to calculate the optical conductivity ( $\sigma(w)$ ) through the relation,  $\sigma(w) = \frac{\epsilon_{im}w}{4\pi}$  with  $w$  being the angular frequency of incident light in radians. The spectral responses of these two parameters are shown in Fig. 4 (a) and (b), respectively. The real part of the dielectric spectra display thickness dependent interesting characteristics presented by broadening and sharp peaks. While the B-band region displays broadens peaks near 3.06 eV, the Q-band region exhibits both broaden and sharp peaks near 1.98 eV and 1.74 eV, respectively.  $\epsilon_r$  values appear to be more sensitive to the film thickness in the Q-band than in the B-band. The critical energies near 3.09 and 1.74 eV is ascribed to the optical transitions in the related bands. It is reported that Zinc phthalocyanine comprises  $18\pi$ -electron structure in the metal free molecule and the zinc- phthalocyanine molecule is very rich in molecular orbitals which result in very dense energy bands [15]. While the ground state of the HOMO (highest occupied molecular orbitals) and SHOMO (singlet highest occupied molecular orbital) are assigned to  $a_{14}(\pi)$  and  $a_{24}(\pi)$ , the first excited LUMO (lowest unoccupied molecular orbitals) level is known to be  $e_g(\pi^*)$  [15, 18]. The electronic transitions from  $a_{14}(\pi)$  to  $e_g(\pi^*)$  result in Q- and B-band absorptions near 2.0 and 3.65 eV. The Q-band splits into two bands centered at 1.75 and 2.0 eV owing to the molecular vibration restrictions in phthalocyanine microcycles [18]. The critical energy at 1.75 eV is

believed to arise from excitonic transitions and/or vibrational conditions [18]. The group of broaden energy peaks in the region of the B-band which is shown by the red colored dotted circle in Fig. 4 (a) should be ascribed to the interactions between ZnPc ( $C_{32}H_{16}N_8Zn$ ) and the  $SiO_2$  rich glass substrate. Transitions in ZnO in the presence of carbon are reported to result in an energy band gap reduction from 3.20 to 3.09 eV [19]. Focusing on  $\epsilon_r$  spectra in the Q-band, it is observed from Fig. 4 (a) that the maximum dielectric constant relate to ZnPc films of thickness of 100 nm. Increasing the thickness of the films furthers to 200 and 400 nm, reduces the value of  $\epsilon_r$  and forces peaks splitting into two peaks centered at 1.76 and 1.62 eV. When the film thickness reaches 600 nm, the peak which appeared at 1.76 increases and the peak which appeared at 1.62 remains as it was.

The optical conductivity spectra for the zinc phthalocyanine which is illustrated in Fig. 4 (b) is considered in the Q-band only. We avoided discussing the B-band region owing to the ZnPc- $SiO_2$  substrate interactions which may be misleading at the current stage. The optical conductivity in the region of 2.8-1.1 eV, exhibits broadens and sharp maxima at 1.98 and 1.77 eV, respectively. In contrast to the behavior of the real part of the dielectric constant,  $\sigma(w)$  spectra are systematic and follow specific trends of variation with increasing thickness. The dependence of the conductivity on the ZnPc film thickness is illustrated in the inset of Fig. 4 (b). The inset of the figure, demonstrates an inverse relation between the optical conductivity and sample thickness. To explore the physical nature beyond this behavior, we have carried out a fitting procedure with the help of Drude-Lorentz approaches for optical conduction in which the optical conductivity takes the form [20, 21]. In the Drude-Lorentz model the optical conductivity takes the form,

$$\sigma(w) = \sum_{i=1}^k \frac{w_{pei}^2 w^2}{4\pi\tau_i((w_{ei}^2 - w^2)^2 + w^2\tau_i^{-2})}. \quad (1)$$

In the above equation,  $w_{pei} = \sqrt{4\pi p_i e^2 / m^*}$  is the plasmon frequency and  $\tau_i = \frac{\mu_i m^*}{e}$  is the scattering time at femtosecond level for a free carrier of concentration  $p_i$ , drift mobility  $\mu_i$  and effective mass  $m^*$ . Here the subscript  $i$  represents the number of oscillators and  $k$  is the number of oscillators at which the series terminates.  $w_{ei}$  is the hole-plasmon reduced frequency in radians. For the zinc phthalocyanine running the series up to  $k = 3$  was sufficient to obtain the experimentally observed conductivity spectra. The reproduced experimental data by Eqn. 1 are shown by black circles in Fig. 4 (b). The good consistency between theory and experiment were achieved through substituting the values of the effective mass of holes as  $13.85m_0$  [22]. Illustrative sample of the obtained optical conductivity parameters for ZnPc films of thicknesses of 50 nm and 600 nm are shown in Table 1.

Table 1. The optical conductivity parameters for ZnPc films.

$i$	$d = 50 \text{ nm}$			$d = 600 \text{ nm}$			$d = 600 \text{ nm annealed}$		
	1	2	3	1	2	3	1	2	3
$\tau(fs)$	1.0	5.3	3.2	0.4	2.6	2.0	0.9	4.0	1.0
$p (\times 10^{20} \text{ cm}^{-3})$	3.8	3.1	2.6	0.3	1.0	1.1	0.30	0.47	2.7
$w_e (\times 10^{15} \text{ Rad/s})$	1.4	2.7	3.0	1.4	2.7	3.1	1.4	2.5	3.0
$w_p (GHz)$	3.1	2.8	2.6	0.9	1.6	1.7	0.9	1.1	2.6
$\mu (\text{cm}^2/Vs)$	0.13	0.68	0.41	0.05	0.33	0.25	0.11	0.51	0.13

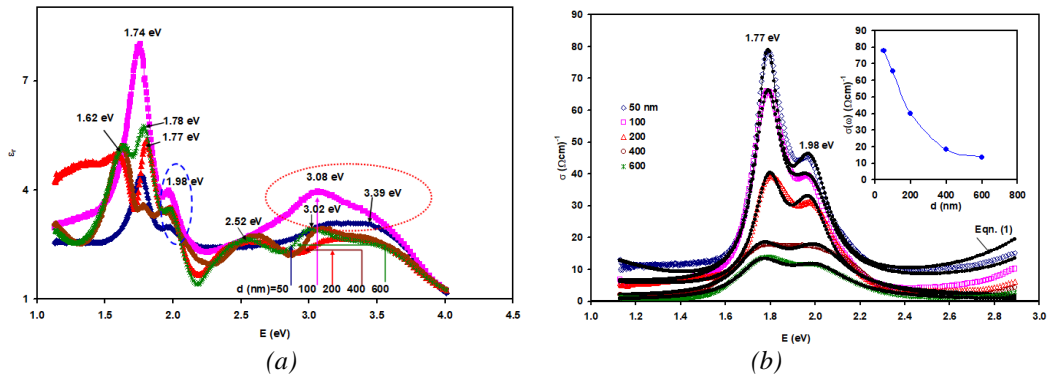


Fig. 4 the thickness dependent (a) real part of the dielectric constant and (b) the optical conductivity spectra for as grown ZnPc thin films. The inset shows the thickness dependence of the optical conductivity at 1.77 eV.

The effect of samples thicknesses on optical conductivity parameters at the absolute maxima of the  $\sigma(\omega)$  spectra (1.77 eV,  $w_{e2} = 2.7 \times 10^{15}$  Rad) are shown in Fig. 5. It is clear from the table that as the oscillator reduced frequency increases from  $1.4 \times 10^{15}$  rad to  $2.7 \times 10^{15}$  rad, the scattering time, the plasmon frequency, the drift mobility and the free carrier concentration increases regardless of the sample thickness. When the hole-plasmon frequency switches to  $3.0 \times 10^{15}$  rad (1.98 eV) from  $2.7 \times 10^{15}$  rad,  $\tau_3$ ,  $w_{p3}$  and  $\mu_3$  decreases and  $p_3$  increases. This observation is valid for all studied samples. On the other hand, considering one particular  $w_{ei}$  value and observing the thickness effect one may observe the variations which are shown in Fig. 5 (a)-(d). As it is clear from Fig.5 (a), the scattering time at femtosecond level which is usually inversely proportional with the damping coefficient decrease with increasing film thickness. It indicates an increase in the damping force which causes electronic friction. The thicker the film, the more rough the surface [23], the larger the scattering. The thicker the film, larger the electronic frictional force, the lower the conductivity [24] (as also shown in the inset of Fig. 4 (b)). It is also observed from Fig. 5 (b), that the free holes density decreases with increasing thickness owing to the increased damping coefficient or decreasing scattering time. It is also noticeable from Fig. 5 (c) and (d) that both of the drift mobility and plasmon frequency decreases with increasing film thickness. The decrease in the values of  $w_p$  with increasing  $d$  values is ascribed to the increased damping coefficient owing to the quadratic relationship ( $w_p^2 \propto p$ ) between the plasmon frequency and the holes density. The drift mobility which is a measure of the drift velocity of free holes per unit electric fields balances the rate of change of the conductivity and free holes density ( $\mu = \sigma(\omega)/(pe)$ ) with thickness. The decrease in the value of  $\mu$  with increasing thickness was previously observed in disordered systems. It is mentioned that in poly(3-hexylthiophene) rectifiers, the effective drift mobility decreases with increasing thickness for the dispersive transport in a disordered system due to the limitations in the free carrier ejection [25]. The decrease in the drift mobility value may also be ascribed to the increased stress with increasing thickness. It is mentioned that, the drift mobility decreases with increasing stress in a manner that depended upon the deformation history [26].

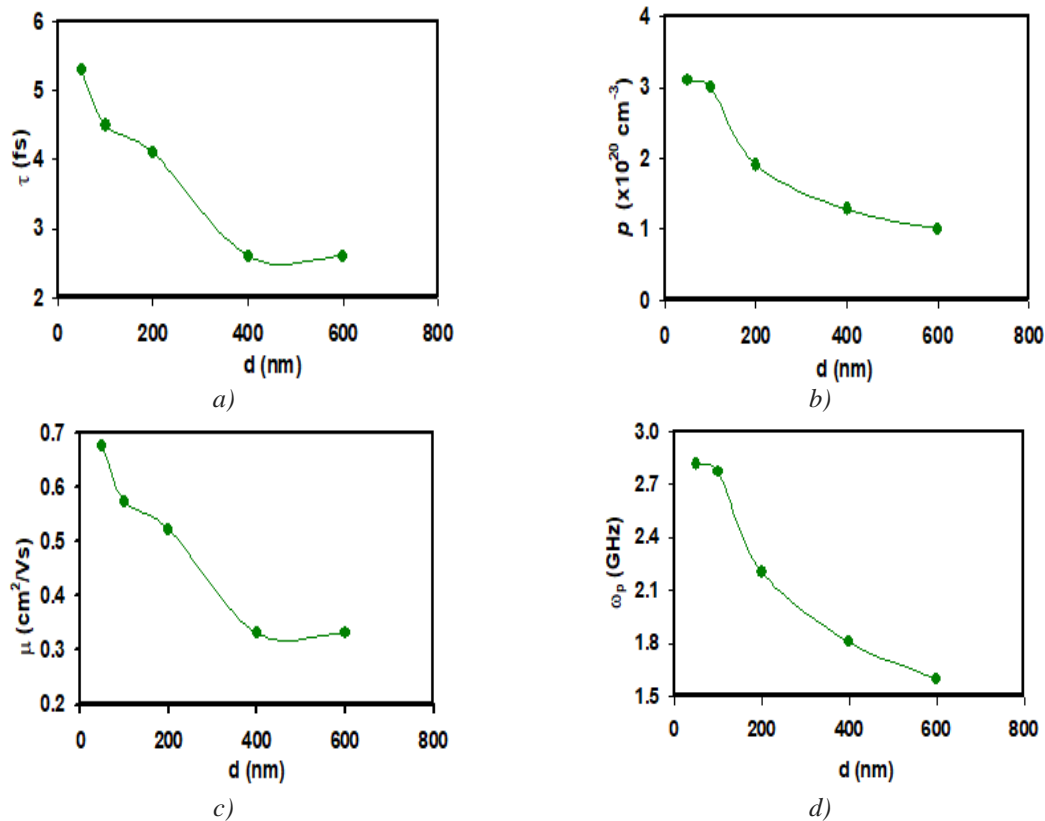


Fig. 5. The thickness dependent (a) scattering time, (b) free hole density, (c) drift mobility and (d) plasmon frequency of as grown ZnPc thin films.

It may be of interest to attract the attention toward the behavior of the optical conductivity parameters under the influence of thin film thickness for oxide materials. Oxide materials like CuO and ZnO display opposite response to that of ZnPc when the scattering time and drift mobility are taken into account [20]. It is reported that, increasing the thickness in CuO decreases the damping factor and results in an enhancement in the drift mobility [20]. However, consistent with our observation in ZnPc, increasing the thickness in CuO decreases the free carrier density and the plasmon frequency. Such behavior was attributed to the increase in the partial pressure of oxygen atoms with increasing film thickness [27].

The effect of thermal annealing of the ZnPc films of thicknesses of 600 nm on the optical properties is illustrated from Fig. 6 (a)-(d). It is clear from Fig. 6 (a) that the absorption coefficient in the B band range is highly influenced by the annealing process compared to the  $\alpha$  -spectra in the Q-band. Namely one may observe an enhancement in the light absorbability in the incident photon range of 3.13-2.17 eV. As for examples, the absorption coefficient values increased by 4.8 times at 2.54 eV. In addition, the plotting's of the absorption coefficient value in accordance with the Tauc's equation for direct allowed optical transitions which is illustrated in Fig. 6 (a) displays  $E$  - axis crossings at 2.91 and 2.60 eV, in the B-band, for the as grown and annealed samples, respectively. The same fitting's revealed a respective decrease in the energy band gap values from 1.60 eV to 1.54 eV in the Q-band. The annealing decreased the energy band gap by 0.31 eV in the B-band and by 0.06 eV in the Q-band. In addition, the dielectric spectra of the real part of the dielectric constant which is illustrated in Fig. 6 (c) mostly display a redshift in the critical energies upon annealing. The absolute maxima in the spectra shift from 1.78 eV to 1.60 eV. The same style of energy shift is also observed in the optical conductivity spectra. As seen from Fig. 6 (d) the maxima of conductivity which was observed at 1.77 eV shifts to 1.65 eV upon annealing. The fitting of the optical conductivity spectra in accordance with Eqn. 1, revealed the optical conductivity parameters which are shown in Table -1. As can be read from the table, the scattering

time and drift mobility increased from 2.6 and 0.33 to 4.0 fs and 0.51 cm<sup>2</sup>/Vs, respectively. The free holes density, the hole-plasmon reduced frequency and the plasmon frequency decreased by 53.0%, 7.4% and by 31.3%, respectively. These significant changes in the optical properties of the ZnPc which is achieved via annealing process, are ascribed to the structural modification that resulted in the poly-crystallization of the material. Earlier studies on the annealing effects on ZnPc films at 200 °C have shown that the material exhibits phase transition from  $\alpha$  to  $\beta$ - phase [28]. The transformation is accompanied with changes in the shapes of grains from spherical to nanorods of length longer than 1.0  $\mu$ m. It was observed that the tilt angle of planar molecules within the columns increases upon annealing. The increase in the tilt angle causes a shortening in the intercolumn distances. It was mentioned that the in-plane ordering of molecules in the nanorods is reached by tight and parallel arrangements of monoclinic cells along the substrate surface leading two low-energy subbands in the Q-band called Q3 and Q4 with stronger electronic coupling in the Q4 band [28]. The process which includes shortening of the  $\pi - \pi$  distance owing to the change in the molecular symmetry of the zinc phthalocyanine may account for the enhanced drift mobility, scattering time and increased light absorbability. Enhanced light absorption coefficient upon annealing at 200 °C was also reported for ZnPc thin films of thicknesses of 750 nm and was ascribed to the phase transition from  $\alpha$  to  $\beta$  and to the compactly stacking of the ZnPc cylindrical clusters along the  $b$  -axes of the monoclinic cell. This type of stacking leads to an overlapping between the ZnPc molecules are much denser way compared to the as grown samples [8].

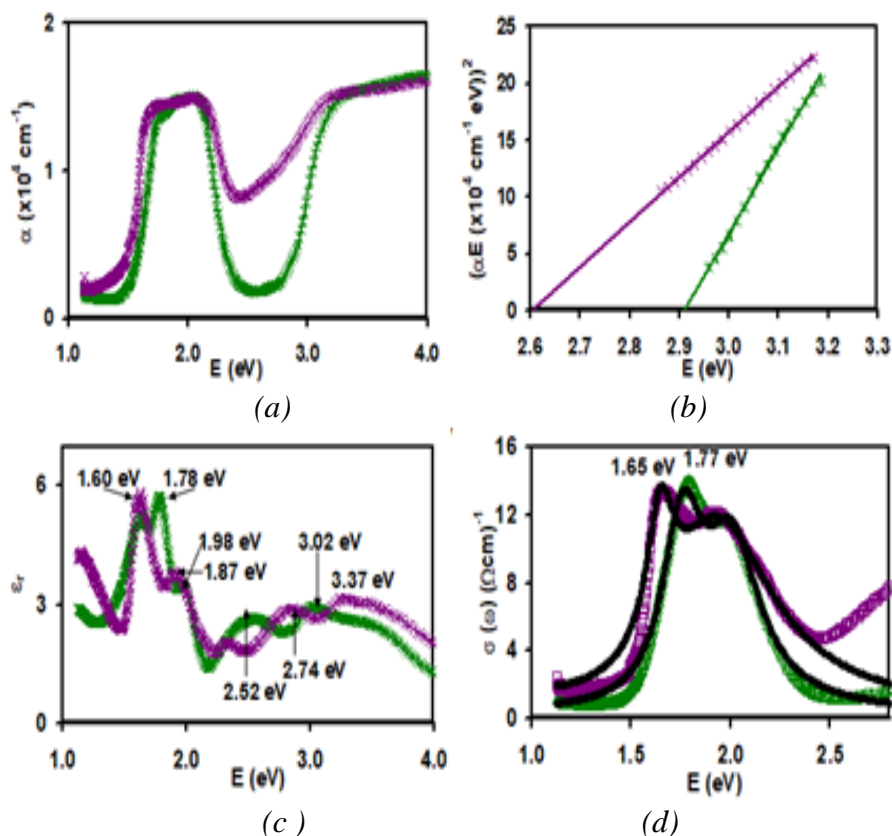


Fig. 6. (a) the optical absorption coefficient, (b) the Tuac's equation fitting, (c) the real part of the dielectric constant and (d) the optical conductivity spectra for the as grown and annealed ZnPc films of thicknesses of 600 nm.

#### 4. Conclusions

In the current study, we attempted to engineer the optical properties and optical conductivity parameters of zinc phthalocyanine via altering the films thicknesses and heat

treatment of some of the films. While increasing the thickness in the range of 50-600 nm lowered the transmittance, redshifts the energy band gap, decreased the all the optical conductivity parameters, the annealing of the thick films (600 nm) in vacuum for one hour at 200 °C enhanced both of the drift mobility and optical absorption coefficient. The optimized features through altering the thickness or annealing the films make the ZnPc thin films more attractive for use in optoelectronic technology owing to large light absorbability in the Q and B band of the light spectrum.

### Acknowledgments

This work was supported by the Deanship of Scientific Research (DSR), University of Jeddah, Jeddah, Saudi Arabia, under grant No. (UJ-02-091-DR). The authors, therefore, gratefully acknowledge the DSR technical and financial support.

### References

- [1] Nicholas T.Boileau, Rosemary Cranston, Brendan Mirka, Owen A. Melville, Benoît H. Lessard, *RSC advances* **9**(37), 21478 (2019).
- [2] Chandan Kumar, Gopal Rawat, Hemant Kumar, Yogesh Kumar, Rajiv Prakash, Satyabrata Jit, *IEEE Transactions on Nanotechnology* **17**, 1111 (2018) .
- [3] Kleyton Torikai, Rafael Furlan de Oliveira, Davi H. Starnini de Camargo, Carlos C. Bof Bufon, *Nano letters* **18**, 5552 (2018).
- [4] Y. S. Zhang, D. X. Wang, Z. Y. Wang, Y. Y. Wang, *Optical and Quantum Electronics* **48**, 18 (2016).
- [5] Anamika Dey, Ashish Singh, Dipjyoti Das, Parameswar Krishnan Iyer, *ACS Omega* **2**, 1241 (2017).
- [6] Miguel Angel Dominguez, Jose Luis Pau, Andrés Redondo-Cubero, *Semicond. Sci. Technol.* **34**, 055002 (2019).
- [7] S. Senthilarasu, Y. B. Hahn, Soo-Hyoung Lee, *Journal of Applied Physics* **102**(4), 043512 (2007).
- [8] S. Senthilarasu, R. Sathyamoorthy, S. K. Kulkarni, *Materials Science and Engineering B* **122**(2), 100 (2005).
- [9] C. Schünemann, C. Elschner, A. A. Levin, M. Levichkova, K. Leo, M. Riede. *Thin Solid Films* **519**(11), 3939 (2011).
- [10] Klyamer, Darya D., Aleksandr S. Sukhikh, Sergey A. Gromilov, Vladimir N. Kruchinin, Evgeniy V. Spesivtsev, Aseel K. Hassan, Tamara V. Basova, *Macroheterocycles* **11**(3), 304 (2018).
- [11] AlGarni, Sabah E., A. F. Qasrawi, *Results in Physics*, 102901 (2019).
- [12] Chiou, Bi-Shiou, Sin-Tah Lin, and Jenq-Gong Duh, *Journal of materials science* **23**(11), 3889 (1988).
- [13] Didier Pribat, Francois Plais, *International Society for Optics and Photonics* **4295**, 60 (2001).
- [14] Xiaodong Ren, Zhou Yang, Dong Yang, Xu Zhang, Dong Cui, Yucheng Liu, Qingbo Wei, Haibo Fan, Shengzhong Frank Liu, *Nanoscale* **8**(6), 3816 (2016):.
- [15] S. Senthilarasu, R. Sathyamoorthy, S. U. B. B. A. R. A. Y. A. N. K. Lalitha, A. Subbarayan, K. Natarajan, *Solar energy materials and solar cells* **82**(1-2), 179 (2004).
- [16] Jacques I. Pankove, *Optical processes in semiconductors*, Courier Corporation, 1975.
- [17] S. M. El-Sayed, G. A. M. Amin, *NDT & E International* **38**(2), 113 (2005).
- [18] Natascha von Morzé, Thomas Dittrich, Wolfram Calvet, Iver Lauer mann, Marin Rusu, *Applied Surface Science* **396**, 366 (2017).
- [19] Ying Zhang, Jiabin Zhou, Xin Chen, Qinqin Feng, Weiquan Cai, *Journal of Alloys and Compounds* **777**, 109 (2019).
- [20] Atef F.Qasrawi, Alaa A. Hamamdah, *Microwave and Optical Technology Letters*.
- [21] M. S. Dresselhaus, M. S. Dresselhaus, J. Tauc, *Optical properties of solids, Part II*,

- book (1998).
- [22] Sukhwinder Singh, G. S. S. Saini, S. K. Tripathi, *Sensors and Actuators B: Chemical* **203**, 118 (2014).
- [23] Xianglin Liu, Lianshan Wang, Da-Cheng Lu, Du Wang, Xiaohui Wang, Lanying Lin, *Journal of crystal growth* **189**, 287 (1998).
- [24] I. Balberg, *Applied Physics Letters* **18**(12), 562 (1971).
- [25] Chan-mo Kang, Seohee Kim, Yongtaek Hong, Changhee Lee, *Thin Solid Films* **518**(2), 889 (2009).
- [26] Hau-Nan Lee, Keewook Paeng, Stephen F. Swallen, M. D. Ediger, *Science* **323**(5911), 231 (2009).
- [27] Holger von Wenckstern, Swen Weinhold, Gisela Biehne, Rainer Pickenhain, Heidemarie Schmidt, Holger Hochmuth, and Marius Grundmann, In *Advances in Solid State Physics*, pp. 263-274. Springer, Berlin, Heidelberg, 2005.
- [28] Hyeyoung Ahn, Ting-Chang Chu, *Optical Materials Express* **6**(11), 3586 (2016).